Nanoscale Fluid Flows in the Vicinity of Patterned Surfaces

Marek Cieplak,[1] Joel Koplik,[2] and Jayanth R. Banavar[3]

[1]*Institute of Physics, Polish Academy of Sciences, Aleja Lotników 32/46, 02-668 Warsaw, Poland*
[2]*Benjamin Levich Institute and Department of Physics, City College of the City University of New York, New York 10031, USA*
[3]*Department of Physics, 104 Davey Laboratory, The Pennsylvania State University, University Park, Pennsylvania 16802, USA*

(Received 7 January 2006; published 23 March 2006)

Molecular dynamics simulations of dense and rarefied fluids comprising small chain molecules in chemically patterned nanochannels predict a novel switching from Poiseuille to plug flow along the channel. We also demonstrate behavior akin to the lotus effect for a nanodrop on a chemically patterned substrate. Our results show that one can control and exploit the behavior of fluids at the nanoscale using chemical patterning.

DOI: 10.1103/PhysRevLett.96.114502 PACS numbers: 47.61.Fg, 47.11.Mn, 47.27.nd, 47.55.D−

Recent advances in fabrication techniques [1,2] have spawned the field of nanofluidics where minute amounts of fluid are contained and controlled for practical use. Here we study fluids of chain molecules flowing in chemically patterned nanochannels [3,4] or placed on a chemically patterned substrate using molecular dynamics simulations. We demonstrate existence of novel flow patterns and find a nanoscale version of the lotus effect [5].

Understanding the behavior of fluids sometimes requires information at the molecular scale, e.g., about the boundary conditions [6]. The continuum description itself may break down as in a rarified fluid in the Knudsen regime [7,8] in which the mean free path is large. Computer simulations bridge molecular scale physics and the continuum behavior [9] and are ideally suited to study nanosized systems. Understanding of liquid and gas flows in nanoscale devices is of great technological interest [1,10] and requires a molecular scale analysis both because the boundary conditions determined by the fluid-solid interactions are all-important and because of dilution.

What are the effects of wettability in the transport of fluids in narrow channels? We consider a fluid comprising small chain molecules in a nanoscale channel with a sharp step in the solid-fluid intermolecular interactions. The nanochannel is bounded by two parallel walls in the x-y plane. Periodic boundary conditions are imposed along the x and y directions. Fluid atoms at a distance r interact with the Lennard-Jones potential $V_{\rm LJ}(r) = 4\epsilon[(\frac{r}{\sigma})^{-12} - (\frac{r}{\sigma})^{-6}]$, where σ is the size of the repulsive core. The potential is truncated at 2.2σ and shifted [11]. The atoms are partitioned into chains of length $n = 10$. The tethering within the chains is provided by the finitely extendable nonlinear elastic potential [12], $V_{\rm FENE} = -(\kappa r_0^2/2)\log[1 - (r/r_0)^2]$, where $\kappa = 30\epsilon$ and $r_0 = 1.5\sigma$ with neighboring atoms of a chain separated by a distance of around σ. The system is maintained at a temperature $T = 1.6\epsilon/k_B$—above the liquid-gas coexistence region of this model. The Langevin thermostat [13] is used with the noise applied in all directions during equilibration and in the y direction afterwords. The radius of gyration of a single molecule in the absence of flow is typically less than 1.7σ. The time unit, $\tau = \sqrt{m\sigma^2/\epsilon}$, where m is the mass of the atom, is of order of 1 ps for typical fluids. The flow is implemented through a ''gravitational'' acceleration of $0.01\sigma/\tau^2$ in the positive x direction. The walls are constructed from two [001] planes of an fcc lattice with a lattice constant of 0.85σ. The wall atoms are tethered to lattice sites by a harmonic spring with a large spring constant. The fluid atoms were confined to a volume of $26.2\sigma \times 5.1\sigma$ in the x-y plane and $L_0 = 12.75\sigma$ between the inner faces of the walls. This corresponds to a channel width of around 4.3 nm for $\sigma = 3.4$ Å, corresponding to liquid argon.

The wall-fluid interactions follow a Lennard-Jones potential $V_{\rm wf}(r) = 16\epsilon[(r/\sigma)^{-12} - A(r/\sigma)^{-6}]$ as in Refs. [8,14]. The parameter A determines the wetting properties of the wall and is varied between 1 and 0 corresponding to attractive and repulsive walls, respectively. We assigned $A = 1$ to the left half of the channel walls and $A = 0$ to the right half. Such a stepwise variation can be accomplished experimentally by coating surfaces with two different kinds of molecules [4]. The number of fluid atoms is equal to 1200 and 240 for the dense and rarified fluids, respectively. In the latter case, only two chains, on average, participate in a ballistic motion at a given instant and the other chains coat the attractive walls. The equations of motion are integrated using a fifth-order predictor-corrector algorithm [13]. The spatial averaging is done in slabs of width $\sigma/4$ along the z and x axes. The rarified fluid data are time averaged over 1×10^6 τ_0 to improve the signal to noise ratio. The error bars are of the size of the data points.

The sharp step in the solid-fluid intermolecular interactions leads to a jump in the wettability, resulting in fluid adsorption and layering on the attractive walls and a cushion of empty space near the repulsive walls [Fig. 1(a)]. The density profiles of the fluid near the walls [Fig. 1(d)] play a key role in determining the flow profile. In contrast to purely repulsive walls [8], the inclusion of regions of the channel wall with attractive interactions results in a flow of the chain-molecule fluid achieving a steady state indepen-

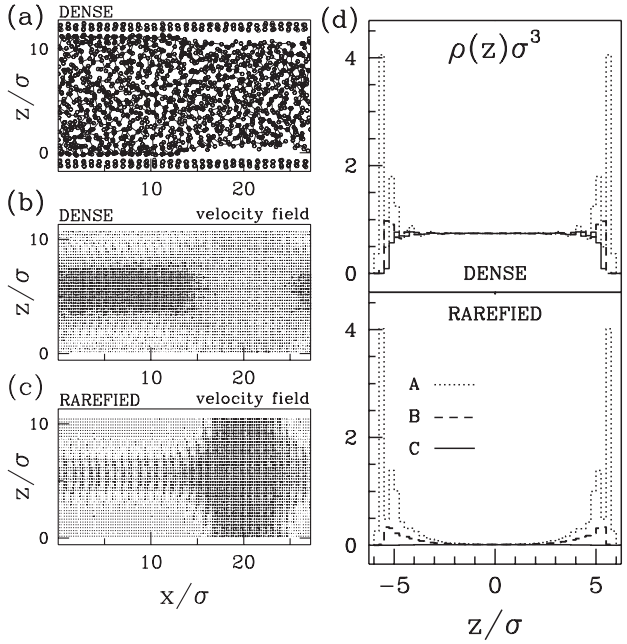

FIG. 1. Molecular configuration, velocity fields, and density profiles of fluids flowing through a patterned nanochannel. (a) A steady state snapshot of the dense system of 120 chain molecules in an x-z projection. (b) and (c) The velocity fields in the x-z plane for the dense and rarefied systems, respectively. The darker vectors represent velocities larger than the average speed at the center point of the system. In (b), the channel effectively widens leading to lower speeds on the right. In (c), the speed is higher in the repulsive region in spite of the increased effective width. (d) The density profiles for the dense (top) and rarefied (bottom) fluids. Three locations along the channel are shown for each case: the dotted, broken, and solid lines are for x/σ around 5.6 (denoted by A), 13.8 (B), and 21 (C) corresponding to attractive walls, the transition region, and repulsive walls, respectively. The atoms of the inner walls are at the edges of the figure. In the wetting region, two monolayers form and make the effective width narrower. In the nonwetting region, the adsorption is absent thus the effective midpoint density falls on moving from A to C. This decrease [not discernible in (d)] is inconsequential for the dense case but explains the anomalous behavior of the velocity field in the rarified case.

dent of fluid density, rather than being accelerated without bounds. The attractive walls provide a mechanism for energy dissipation which is absent when walls are all repulsive. (Interestingly, monatomic fluids do reach a steady state in the presence of such walls). For the flow rates considered here (Re ~ 3 and 8 in the dense and rarefied cases, respectively), the conformations of molecules are fairly isotropic at the center of the channel but elongated along the flow direction at the attractive walls. More strikingly, the character of the flow itself changes depending on the location of the channel and the nature of the wall-fluid interactions. Furthermore, the velocity fields are distinct for the dense fluid and in the Knudsen regime [Figs. 1(b) and 1(c)].

The velocity profiles [Fig. 2(a)] of the nanoflows exhibit the expected Poiseuelle character in the region of the channel with attractive walls but one obtains a plug flow in the region bounded by purely repulsive walls. Note that the speed of the plug flow is smaller than the peak velocity of the Poiseuelle flow in the dense fluid case while the opposite behavior holds for the rarified fluid, underscoring the important role played by fluid-fluid interactions in controlling the dissipation. Indeed, in the Knudsen regime, the fluid molecules in the region bounded by repulsive walls undergo free acceleration with a moderating dissipation occurring only when they pass through the region with attractive walls, resulting in a stationary state. Figure 2(b) shows the slip length [7,8,15] and 2(c) the maximum

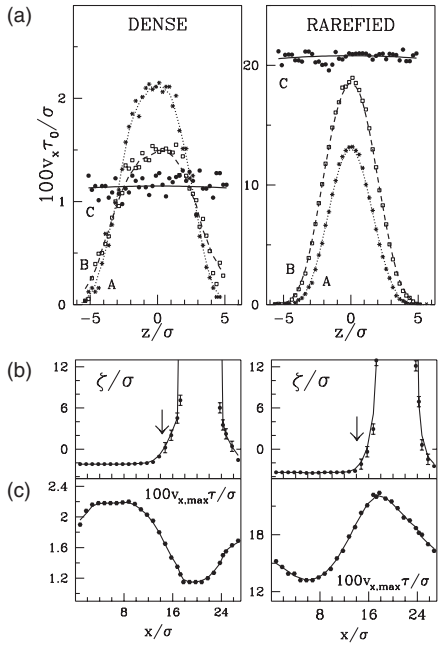

FIG. 2. Nanoflow attributes for the dense (left panels) and rarefied (right panels) regimes. (a) The velocity profiles for the x components of the flow velocity as averaged in strips located at points A (asterisks), B (squares), and C (circles) as in Fig. 1(d). The lines are guides to the eye. One sees the Poiseuelle parabolic flow at A and B changing to plug flow at C. Dissipation at the attractive walls leads to stationarity of the flow that is missing for purely repulsive walls. (b) The slip length, ζ, along the length of the channel. The arrow shows the location of the switchover in wettability. ζ is obtained as a linear extrapolation of the flow profile and is a measure of the distance from the wall at which the extrapolated velocity vanishes. Positive (negative) ζ indicates that the extrapolated velocity vanishes outside (inside) the channel. ζ is negative for the attractive region but becomes positive and large when the fluid is within repulsive walls. The effective viscosity, as measured from the curvature of the velocity profiles at the midpoint of the channel, is also a function of location along the channel and it follows the behavior of ζ. (c) The maximum velocity, $v_{x,\max}$, occurring halfway between the walls, as a function of x. It grows on crossing the wettability step in the rarefied case but decreases in the dense case.

velocity in different parts of the chemically patterned channel.

We have also studied channels that are patterned geometrically with homogeneous attractive wall-fluid interactions. The extra space in the wider fragments of the channel gets filled in by fluid molecules and the resulting flow is similar to that in a uniform width channel, underscoring the important role played by the wetting heterogeneities compared to structural patterning. Earlier studies [16] had considered a similar geometrically patterned channel but with uniformly repulsive walls leading to large slip and low flow resistance, akin to the uniform channel case.

We turn now to the study of the behavior of a fluid nanodroplet on a substrate [17]. The droplet (Fig. 3) is made of 1800 fluid atoms resting on the bottom wall of the channel. The reduced temperature is chosen to be 0.8 so that the vapor pressure is essentially zero. The shape of the droplet on a surface is determined by the balance between the interfacial energies of the interfaces involved. In our simulations there is a minimum wall-fluid attraction, A, that is required to hold the droplet on the substrate. This value, found to be around $A = 3/8$, separates two cases—for $A > 3/8$, the droplet stays on the substrate and otherwise it detaches. Our first set of runs were carried out with a homogeneous substrate characterized by this threshold value of A. The contact angle that one obtains is around $110° \pm 10°$.

In order to assess the effects of the chemical patterning, we considered a modified substrate in which the previous value of A was restricted to periodically repeated square patches placed in the background with an even smaller value of $A = 1/4$. The ratio of the patch size (3.4σ) to the droplet diameter (16σ) and the strength of the interaction with the background were chosen so that the static drop was barely attached to the substrate. The pattern leads to an increase in the contact angle (to $130° \pm 10°$) without compromising the stability of the fluid on the substrate.

In the presence of a lateral push due to a small applied acceleration the drop on the homogeneous substrate has insignificant center-of-mass motion whereas the drop on the patterned substrate readily responds to the push with a combination of rolling and diffusive motions (Fig. 4). This behavior is akin to the lotus effect [5] but on a nanoscale.

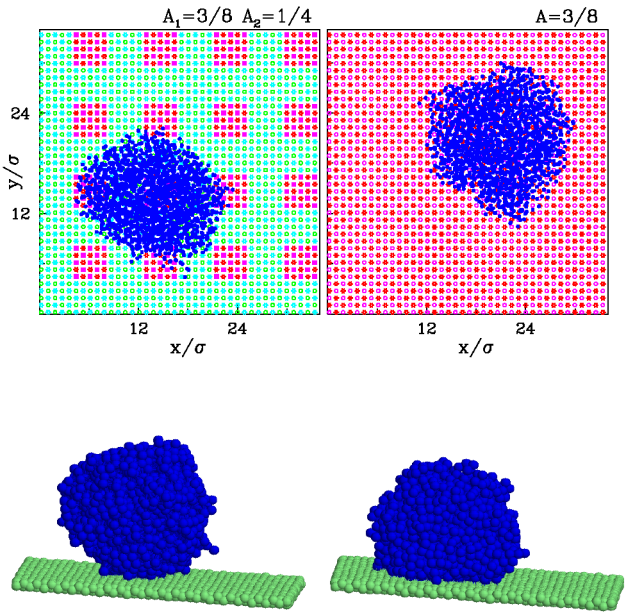

FIG. 3 (color online). Snapshots of droplets on a solid substrate. The pictures show a view (projection) from the top and a three-dimensional depiction of the droplet in a side view (bottom). The left pictures refer to a patterned substrate with periodic squares with $A = A_1 = 3/8$ superposed on a background of $A = A_2 = 1/4$ while those on the right depict a homogeneous surface with $A = 3/8$ corresponding to partial wetting. Smaller values of A typically lead to the detachment of the droplet. The choice of the A_1 and A_2 coefficients was dictated by the requirement of marginal attachment. Note that the contact angle is larger for the patterned substrate resulting in "superhydrophobicity." In some of our runs with the patterned substrate, the droplet detaches when pushed laterally.

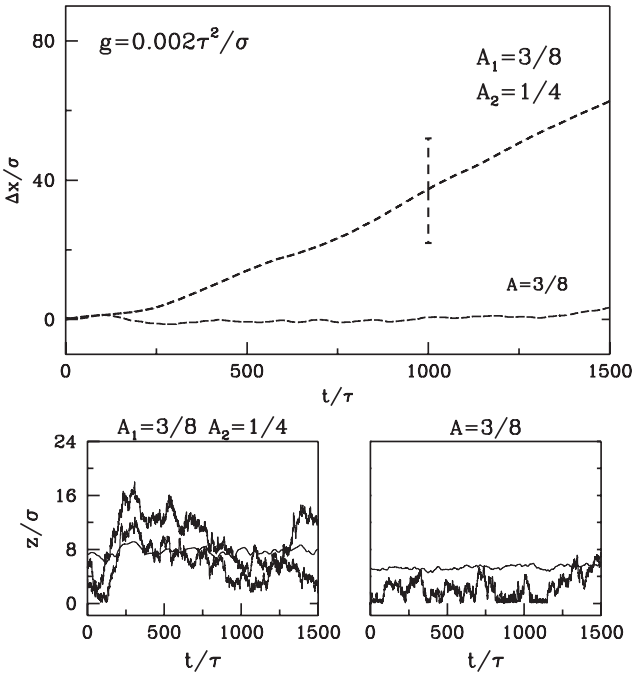

FIG. 4. The "lotus" effect. Top: the time dependence of the longitudinal displacement of the center of mass of the droplets pushed with $g = 0.002\tau^2/\sigma$ along the x direction averaged over four runs. For the homogeneous substrate the droplet hardly moves but the motion is rapid for the patterned substrate. Bottom: the time dependence of height z above the substrate of droplet atoms (two on the left, one on the right) which are initially close to the surface of the droplet and the wall. The nearly horizontal line indicates the location of the center of mass of the droplet and provides a reference. The pictures suggest rolling motion [18] combined with diffusion for the patterned substrate (left) and pure diffusion for the homogenous substrate.

The lotus leaf is self-cleansing because water droplets roll off easily and collect dirt, due to an interplay between its rough microstructure and its tendency to repel the water. In our case, a similar effect at the nanoscale occurs even for a smooth substrate but with heterogeneous wetting properties.

We have shown that molecular dynamics simulations can be used to elucidate boundary conditions, flow profiles in a patterned channel, and an analog of the lotus effect, demonstrating novel behaviors that one may observe in the nanoworld. Controlling and harnessing fluids at the nanoscale through chemical patterning may offer new opportunities in science and technology.

We would like to acknowledge stimulating discussions with Amos Maritan and Giampaolo Mistura. This work was supported by Ministry of Science in Poland (Grant No. 2P03B-03225), the NASA Exploration Systems Mission Directorate, and by the European program IP NaPa through Warsaw University of Technology.

[1] G. M. Whitesides and A. D. Stroock, Phys. Today **54**, No. 6, 42 (2001); S. Casimirius, E. Flahaut, C. Laberty-Robert,
L. Malaquin, F. Carcenac, C. Laurent, and C. Vieu, Microelectron. Eng. **73–74**, 564 (2004).

[2] S. D. Gillmor, A. J. Thiel, T. C. Strother, L. M. Smith, and M. G. Lagally, Langmuir **16**, 7223 (2000); A. A. Darhuber, S. M. Troian, J. M. Davis, and S. M. Miller, J. Appl. Phys. **88**, 5119 (2000); T. P. Russell, Science **297**, 964 (2002).

[3] P. E. Laibinis, R. G. Nuzzo, and G. M. Whitesides, J. Phys. Chem. **96**, 5097 (1992); P. A. Lewis *et al.*, Nanotechnology **12**, 231 (2001); P. S. Swain and R. Lipowsky, Langmuir **14**, 6772 (1998).

[4] T. Auletta *et al.*, Angew. Chem., Int. Ed. **43**, 369 (2004).

[5] W. Barthlott and C. Neinhuis, Planta **202**, 1 (1997); A. Marmur, Langmuir **20**, 3517 (2004); R. Blossey, Nat. Mater. **2**, 301 (2003).

[6] J. C. Maxwell, Phil. Trans. R. Soc. London **170**, 231 (1879).

[7] E. H. Kennard, *Kinetic Theory of Gases* (McGraw-Hill, New York, 1938).

[8] M. Cieplak, J. Koplik, and J. R. Banavar, Phys. Rev. Lett. **86**, 803 (2001); M. Cieplak, J. Koplik, and J. R. Banavar, Physica (Amsterdam) **287A**, 153 (2000).

[9] B. J. Alder and T. E. Wainwright, Phys. Rev. Lett. **18**, 988 (1967); J. Koplik and J. R. Banavar, Annu. Rev. Fluid Mech. **27**, 257 (1995).

[10] T. M. Squires and S. R. Quake, Rev. Mod. Phys. **77**, 977 (2005); J. Atencia and D. J. Beebe, Nature (London) **437**, 648 (2005).

[11] P. A. Thompson and M. O. Robbins, Phys. Rev. A **41**, 6830 (1990).

[12] M. Kroeger, W. Loose, and S. Hess, J. Rheol. (N.Y.) **37**, 1057 (1993).

[13] M. P. Allen and D. J. Tildesley, *Computer Simulation of Liquids* (Clarendon, Oxford, 1987).

[14] J. L. Barrat and L. Bocquet, Phys. Rev. Lett. **82**, 4671 (1999).

[15] T. Schmatko, H. Hervet, and L. Leger, Phys. Rev. Lett. **94**, 244501 (2005).

[16] C. Cottin-Bizonne, J. L. Barrat, L. Bocquet, and E. Charlaix, Nat. Mater. **2**, 237 (2003).

[17] D. Queree, Nat. Mater. **1**, 14 (2002); A. Lafuma and D. Quere, Nat. Mater. **2**, 457 (2003); S. Daniel, M. K. Chaudhury, and J. C. Chen, Science **291**, 633 (2001).

[18] L. Mahadevan and Y. Pomeau, Phys. Fluids **11**, 2499 (1999).